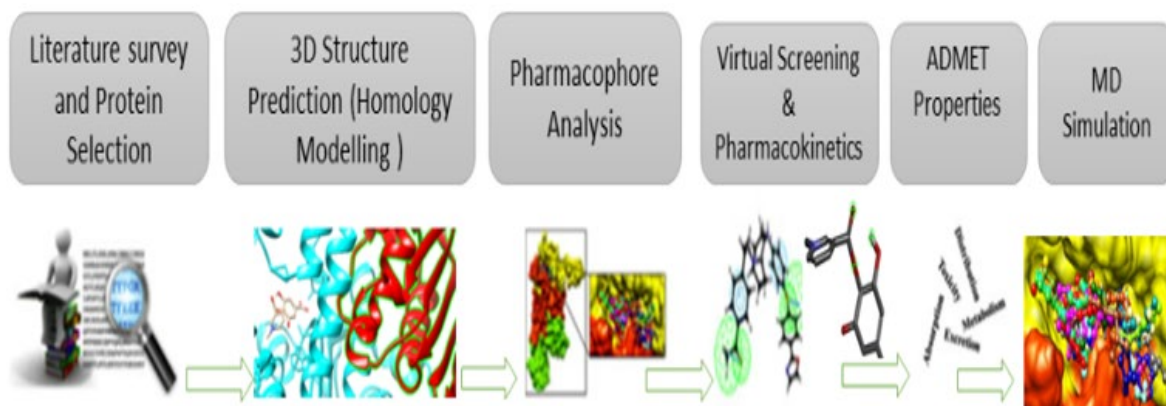


Computational Analysis and Phytochemical Screening Targeting Dihydrolipoamide Dehydrogenase (DLD) for Alzheimer's Disease: A Molecular Dynamics Simulation Study

Muhammad Mazhar Fareed

School of Science and Engineering, Department of Computer Science, Università degli Studi di Verona, Verona, Italy E-mail: muhammadmazhar.fareed@studenti.univr.it

Abstract: The decreasing rate of metabolisms within the mitochondrial is connected to the progressive characterization of Alzheimer's Disease (AD). Dihydrolipoamide dehydrogenase (dld), and DLD1 are specific chemicals comprised of two enzymes/complexes of protein; pyruvate dehydrogenase and α -ketoglutarate dehydrogenase physiologically related to AD and have a noteworthy function in energy metabolism. The present computational study was designed to envisage a rational screening of natural phytochemical compounds against DLD1 in AD. The molecular docking and virtual screening approaches were adopted within the best binding active sites of DLD1 in AD to screen 15,282 medicinal phytochemicals' libraries, which were developed from the literature search, PubChem, Zinc Database, and MPD3 Database. This docking followed by MD-simulation of the best three complexes (1-Caffeoyl-4-deoxyquinic acid, N-Butyryl Coenzyme A, Precatorine) determined through docking scores, RMSD-refine, Pharmacokinetics properties, pharmacological analysis, molinspiration, ADMET-properties, and binding energies. The top complexes with docking-S scores (-13.7117, -12.4565, -11.6440), RMSD-refine values (1.64, 0.86, 0.93), and interactive hits/residues (Arg216, Leu263, Ile125, Met262, Asp256), showed a binding affinity with another catalytic active site domain-chain A (residues 86-293). Although this *in-silico* work is not experimentally determined, the affinity and interactions of these selected novel compounds might help to design the therapeutics against Alzheimer's Disease.



Graphical research abstract

Keywords: Alzheimer's disease, Dihydrolipoamide dehydrogenase (DLD1), Molecular docking, Natural medicinal compounds, MD-simulation, Pharmacokinetics analysis.

Doi: [10.5281/zenodo.12683808](https://doi.org/10.5281/zenodo.12683808)

1. Introduction

Alzheimer's disease is an ordinary form of dementia that resembles Parkinson's disease, analogous to chronic neurodegeneration. Formerly, the ratio of AD infections is up to 46 million and is expected to be 100M in 2050 if effective treatments are not discovered. AD was nominated by the name of German clinical psychiatrist and neuroscientist Alois Alzheimer (Reitz & Mayeux, 2014). When, in 1901, a prolonged investigation of a female patient dominated signs of confusion, aggression, paranoia, and memory disturbance (Wimo et al., 2017). In 1996, a female patient with Alzheimer's disease in her post-mortem report dominated the presence of plaques and neurofibrillary tangles (NFTs) in her brain. The excess in glucose levels accompanying metabolism is a major pitfall of AD (Zhang et al., 2011; Zhang et al., 2012; Ling, Morgan and Kalsheker, 2003; Nag et al., 2011; Giuffrida et al., 2009). The enhancement of AD symptoms under caloric restriction and reducing glucose is majorly dependent on metabolism (Taylor et al., 2010; Zhang et al., 2015; Wang et al., 2014).

There are two primary schools of thought regarding the cause of AD, enlisted first is the production and deposition of AD from A β -cleavage amyloid-beta precursor protein that participates in neuronal protein trafficking, calcium mesoblast, cell adhesion as well as transmembrane signal transduction. Where A β is 39-42 residue peptide originated after sequential breakage of APP by γ -secretase complexes. The APP cleavage by α -excretase use evolved in the origination of large and soluble ectodomain of APP (sAPP α). Unrestricted production and defective A β clearance lead to AD by blocking neurotransmission, reducing neutral synapsis as well as promoting mitochondrial dysfunction (Wang et al., 2015; Ballatore et al., 2007). Second is the commencement of synaptic loss and neural degeneration in AD due to the initiation of NFTs. NFTs are caused due to obstruction of mitochondria leading to the disarranging of the neuronal cell body structure in AD (Wang et al., 2013; Völgyi et al., 2017).

DLD/DLD1 (Dihydrolipoamide dehydrogenase, dihydrolipoyl dehydrogenase), is a mitochondrial enzyme paramount for energy metabolism in the TCA cycle (tricarboxylic acid cycle, citric acid cycle (CAC)) of AD. DLD1 is the core enzyme in AD. Mainly DLD1 is a subunit of ketoacid dehydrogenase complexes each promoting energy metabolism, α -ketoglutarate dehydrogenase complex (KGDH), pyruvate dehydrogenase (PDH), glycine cleavage system (GCS), and branch-chain ketoacid dehydrogenase complex (BCKDH). Under the Alzheimer's or Parkinson's post-mortem report, it seems that the depletion in the venture of PDH and KGDH is correlated, also with neurodegeneration causing complexities in brain tissues and fibroblasts (Yao et al., 2011; Brown et al., 2007; Carothers et al., 1989). Neuro-DLD activities lead to low glucose metabolism whereas, pyruvate dehydrogenase and α -ketoglutarate dehydrogenase play a vital role in energy metabolism Yao et al., 2011; Brown et al., 2007; Carothers et al., 1989; Vilalta et al., 2014).

The Dysfunction of mitochondria in Alzheimer's disease and diabetes is linked with DLD1 in NFTs and A β 's initiation in AD, as well as Human islet amyloid polypeptide (hIAPP) and insulin resistance in diabetes, are attributes for disease as insulin signature also leads to neurodegeneration and cognitive mutation (Gibson et al., 1998). Moreover, mitochondrial dysfunction increases oxidative stress. Both AD and diabetes are degenerative diseases involved in β -cells destruction, and the neuronal loss system, respectively. The main systematic link between these diseases is impaired signaling of insulin leading to cognitive neurological damage and neurodegeneration (Shi et al., 1782; Ristow et al., 2004; Sun, M.-K. Sun and Alkon, 2006). In addition to sharing the same pathways in AD and diabetes types-3, and also share several enzymes in common such as; glutamic acid decarboxylase, dopa-decarboxylase,

growth receptors factors; p75-receptors, neuronal growth factor receptors (NGFR) and thyrotropin-releasing hormone (TRH), and second messenger abnormalities (SMA), glycogen synthase kinase-3 (GSK3) overactivity, dysregulated protein phosphorylation (DPP) in metabolic activities (Ott et al., 1999; Hoyer, 2004; Hoyer and Nitsch, 1989; Perry and Greig, 2002).

As we know, oxygen and nutrients are utilized by aerobic organisms for energy production in ATP. In the DLD1 mechanism of AD 90% of cellular ATP is mitochondrial production by oxidative phosphorylation in metabolic reactions. On the other hand, neuron performance requires the bulk of energy, and neuronal cells' limited glycolytic diversion makes them mitochondrial-dependent. So, the AD-related report revealed that abnormalities such as calcium homeostasis, and oxidative stress are the result of mitochondrial impairment causing neural dysfunction and neurodegeneration (Mattson, 2008; Moreira, 2009).

Medicinal-like Phytochemicals are extracted from medicinal plants (Yadav and Agarwala, 2011), which are of two categories; primary, and secondary phytochemicals; primary comprises proteins, chlorophyll, amino acids, and starch-sugars, and secondary constituents are flavonoids, steroids, alkaloids, phenols, terpenoids, tannins, anolides, antimetabolites, riboflavin, saponins, and pectin-like chemicals (Mukhtar et al., 2008). Phytochemicals are mainly used for the biological cure specifically for antifungal, anti-viral activities, anti-inflammatory, and anti-neural progression response (Wadood et al., 2013; Hussain et al., 2011; Eleazu et al., 2012; Grassi et al., 1998; Farquar, 1996; Chandel et al., 2020; Wang et al., 2020; Naithani et al., 2008).

In-silico computer-aided drug design (CADD) has a key role in drug discovery, design, and chemical and biological information about interactions of ligands, and has been used to investigate biological queries via; using mathematical and computational techniques X-ray crystallography, NMR (nuclear magnetic resonance), which is very time-consuming, costly for protein modeling. The high-throughput screening analysis of small chemical compounds against the target receptor is also very expensive (Nobile et al., 2017; Mandal and Mandal, 2009).

In this study, we predicted the 3D structure of DLD1 and executed an MD Simulation of the hit complex using *In-silico* bioinformatics approaches. The main objective/aim of our research work is to elucidate the interaction between the top best-screened ligands with DLD1 protein. Hence, this present research was carried out to provide molecular-based interaction insight into

the DLD1 protein structure, and to discover its most potential natural therapeutics drugs, with plausible functionality of DLD1 against AD.

2 Methodologies and Materials:

2.1 Data Collection of DLD1 in Alzheimer's Disease

The sequence of DLD1 (accession no: P09622) was downloaded in FASTA Format from the UniProt Knowledgebase database (Consortium, 2015).

2.2 Structure Prediction Analysis

The protein structure of DLD1 (UniProt accession no: P09622) was predicted from RaptorX, SwissModel (Källberg et al., 2012), and this analysis was done through UCSF-Chimera version 1.4.1 and PyMol version 2.3.3 (Pettersen, 2004; Lill and Danielson, 2011).

2.3 Structure Evaluation of DLD1

Different evaluation tools were used for the evaluation of the protein structure of DLD1. The models are generated by RaptorX; the model was selected based on Verify3d, Molprobability, and Rampage results. The quality of the 3D model was confirmed by Verify3D (Eisenberg, Lüthy, and Bowie, 1997; Wang et al., 2016). Rampage generated a Ramachandran plot for the assessment of models along with the allocation of residues in allowed, outliers, and favored regions (Wang et al., 2016).

2.4 Active Sites Prediction of DLD1 in AD

The binding pockets containing key residues of DLD1 were predicted through meta-COACH-server (Yang, Roy, and Zhang, 2013), and structural proteins' molecular functional residue sites were predicted through ExpASY-ProSite/ScanProSite (Gasteiger et al., 2003). The physicochemical properties of DLD1, such as; atomic and amino acid composition, grand average of hydropathicity (GRAVY), instability-index & isoelectric point were using of ProtParam tool of ExpASy (Gasteiger et al, 2003), and dld1 protein-domain were predicted through Pfam (Bateman, 2004).

2.5 Structural refinement and energy minimization DLD1 in AD for molecular docking

The generated structure of the DLD1 was minimized through the UCSF-Chimera version 1.4.1 visualizing tool by selecting the steepest steps (1000), conjugate gradient steps (1000), and adding the Gasteiger and hydrogen charges to remove clashes and unnecessary atoms from

(Ashfaq et al., 2013), MPD3-databases (Irwin and Shoichet, 2005), Zinc databases (Bolton et al., 2008), PubChem (Ashfaq et al., 2013), and Drug bank (Mumtaz et al., 2017) in SDF file format and prepared ligand by adding hydrogen charges, through protonate 3D, energy minimization was done via selecting MMFF94x Force-Field (Wishart et al., 2018), in MOE (Vilar et al., 2008), and edit these ligands to the MOE databases for the molecular screened against DLD1 in AD, and the top selected ligands in SDS-File was downloaded through PubChem-Database are shown in Figure 02 (Kim et al., 2016).

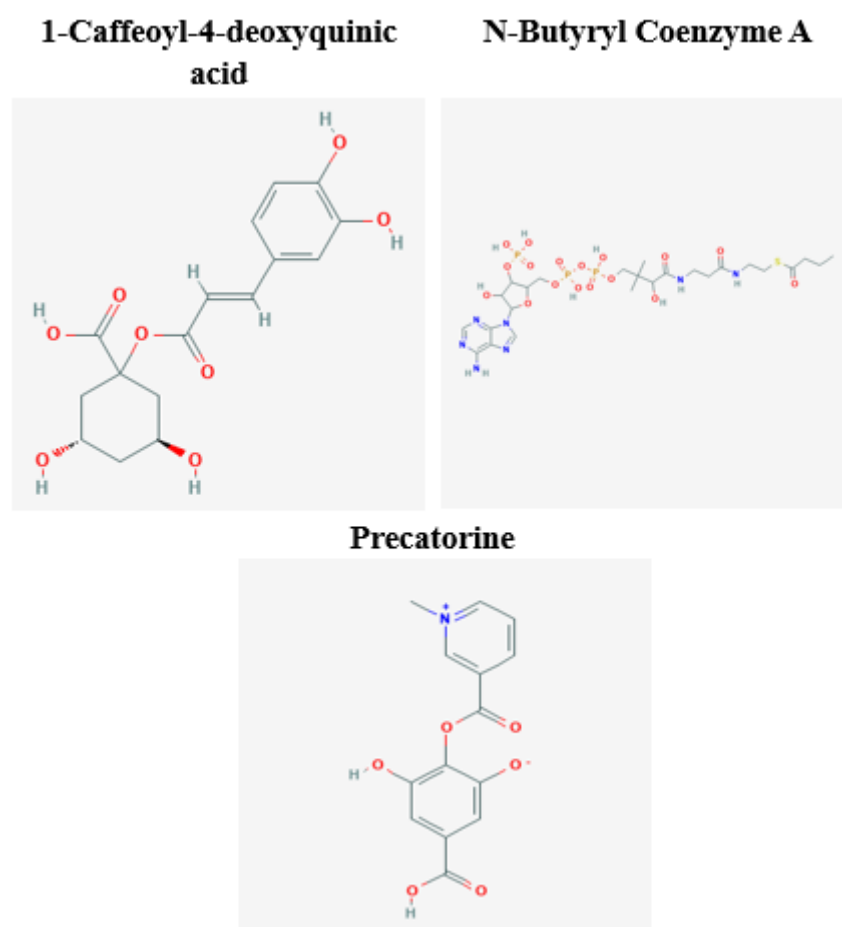


Figure 02: Top 03 ligands figure against the DLD1 in AD through PubChem Tool (<https://pubchem.ncbi.nlm.nih.gov/>)

2.8 Molecular docking

The virtual screening of the compounds was applied to the library of 15,282 phytochemicals. The virtual screening was applied using the molecular docking approach through MOE (Farag et al., 2020), and PyRx tool (Chandel et al., 2020), The targeting molecular docking approach was used to screen the potential drugs targeted based inhibitor as top-compounds against DLD1

through PyRx (Dallakyan and Olson, 2015). The pharmacophore-based selected top-hit compounds with optimum binding energies were selected by PyRx (Dallakyan and Olson, 2015) and visualization of the top binding residue was executed through LigX of MOE (Hosseinzadeh, Mazaheri, and Ghodsi, 2017).

2.9 Pharmacokinetics analysis

The molecular-based physiochemical properties and drug likeliness properties of best docking phytochemicals were analyzed using the tool Molinspiration server (Reena Roy, Kandagalla, and Krishnappa, 2020), which gives a prediction results 'rule of five' (Ro5) based on molecular properties such as; H-bond-acceptors fewer as less than 10, less than 05 H-bond-donors, MloP value less than 05%, and a molecular weightless and equal 500 (Daltons) (Adhikari et al., 2020). Further, the quantitative analysis including ADMET profiling of top selected compounds was *in-silico* based observed through SwissAdme (Daina, Michielin, and Zoete, 2017; Cheng et al., 2012; Patel et al., 2020). and the selected compounds' bio-activity was analyzed through Molinspiration (Wadapurkar, 2018). The DLD1 gene association with enzymatic properties was predicted through the BRENDA Database, ExplorENZ-Enzyme database (Schomburg et al., 2004; McDonald, Boyce, and Tipton, 2009).

3. MD-Simulation

The validation of docking was done via MD simulation using the Desmond v3.6 version (Shivakumar et al., 2010). For this purpose, MD simulation was carried out using the model namely TIP3P (transferable intermolecular potential with 3 points) accompanied by a boundary box of an orthorhombic-shaped. The stability of the protein-ligand interactions was acquired with the OPLS-2005 (optimized potential for liquid simulation) force field incorporating sodium ions. The minimization step was acquired through algorithms including the steepest descent (SD) method and LBFGS of the protein-ligand system. The MD simulation was run with 100ns via Desmond software to scrutinize the complexes of protein-ligand, acquired from docking (Shivakumar et al., 2010).

4. Results and Discussion

4.1 Structure Evaluation of DLD1

The evaluation tools indicated the efficacy and reliability of the predicted structure of DLD1 in AD through the Ramachandran plot (Molprobability-Rampage) that showed the presence of residues with a percentage of 98.28% in favored regions, the residues in the outlier region were observed at 0.00%, Rama distributed Z-score with -0.57 to $0.28 < 2$ also along with favored rotamers 95.52% (98.3% (802/816) of all residue were in (98%) favored regions, 100.0% (816/816) of all residues were in ($>99.8\%$) allowed regions, also there were no outliers regions) along with psi, and phi (Ψ , ϕ or ϕ) angles. Verify3D showed an overall quality factor of 81.95% of the residues with has averaged 3D-1D score ≥ 0.2 , and at least 80% of the amino acids have scored ≥ 0.2 in the 3D/1D profile of DLD1 are shown in Figure 3.

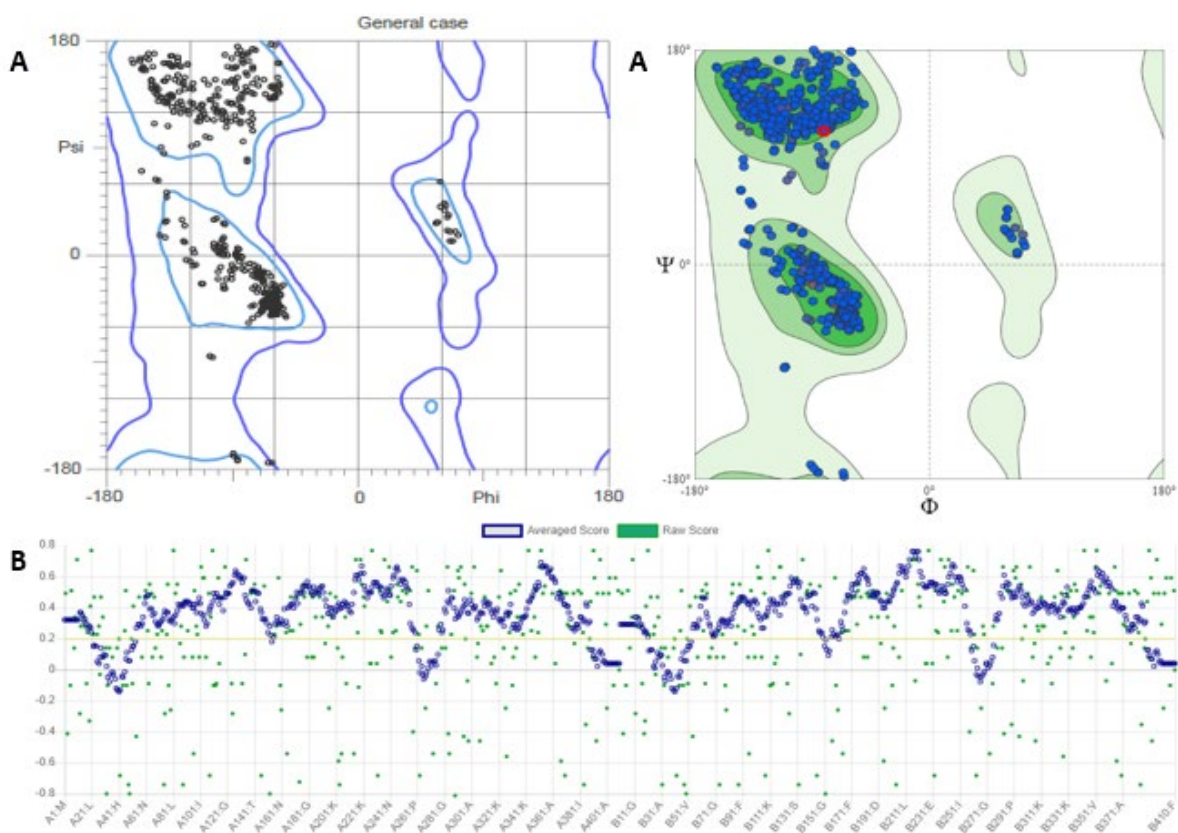


Figure 3: Results of Molprobability Rampage (A), and Verify3D (B), the structure evaluation of the DLD1 in Alzheimer's Disease.

4.2 Active Sites Prediction of DLD1 in AD

The DLD1 binding-pocket residue was predicted and selected through TM-Sites of the Meta COACH-server. The Physiochemical properties of DLD1 were predicted through the ExpASy-ProtParam tool (Garg et al., 2016). The analysis revealed physiochemical properties such as a DLD1-protein length was 410 amino acids having 43587.12 Dalton molecular weight. The

GRAVY score and instability index were computed as -0.036 and 92.51 classifying the protein as stable protein depicting those hydrophilic residues can establish hydrogen bonds are shown in Table 1, and the DLD1 protein domain predicted through Pfam (Bateman et al., 2004), results show that the families (pyridine nucleotide-disulfide oxidoreductase, dimerization domain of dld1) included both class1 and class2 oxidoreductases, and also NADH oxidases and peroxidases with domain a small binding within a larger FAD binding domain. The observed protein domain values are the results; pyr redox-2 starts domain 42 to end domain 370, and pyr redox dim starts 389 to end domain 410, and the E-values of sequence 1.6e-62, domain 1.6e-62, sequence of domain values are 7.5e-39, 2,7e-38 were identified.

Table 01: Physicochemical parameters of DLD1 in Alzheimer's disease

Parameters	DLD1 in Alzheimer's disease
Mol. Weight	43587.12
No. of amino acids	410
Theoretical <i>pI</i>	6.57
Instability index (II)	26.00
No. of Negatively Charged Residues (Asp+Glu)	48
No. of Positively Charged Residues (Arg+Lys)	46
Aliphatic Index	92.51
Grand average of Hydropathicity (GRAVY)	-0.036
Atomic Composition	Carbon C 1926 Hydrogen H 3119 Nitrogen N 531 Oxygen O 585 Sulfur S 16
Amino Acid Composition	Ala (A) 39 9.5%, Arg (R) 13 3.2%, Asn (N) 16 3.9%, Asp (D) 19 4.6%, Cys (C) 6 1.5%, Gln (Q) 11 2.7%, Glu (E) 29 7.1%, Gly (G) 47 11.5%, His (H) 10 2.4%, Ile (I) 32 7.8%, Leu (L) 27 6.6%, Lys (K) 33 8.0%, Met (M) 10 2.4%, Phe (F) 14 3.4%, Pro (P) 13 3.2%, Ser (S) 20 4.9%, Thr (T) 25 6.1%, Trp (W) 2 0.5%, Tyr (Y) 6 1.5%, Val (V) 38 9.3%, Pyl (O) 0 0.0%, Sec (U) 0 0.0%

4.3 SVM domain protein analysis

The SVM-Domain linker prediction (DLP) domain protein analysis of the DLD1 in AD favorite candidate region prediction as output values/length with the Threshold SVM1-All

0.00, SVM-Long 0.00, SVM-Short -0.50, Offset SVM-All 40, SVM-Long 40, SVM-Short 40, and the number of predicted regions result; Ranks SVM-All 02, SVM-Long 02, SVM-Short 02. The candidate regions SVM-All with peak values of 1.129, 1.022, peak position 90, 237, region 85-96, 231-245 with sequence GSEVTPFPGITI, ELDPGRIPVNTRFQ, SVM-Long with peak-value 1.303, the position of peak 237, region of protein 228-246 also with LGIELDPRGRIPVNTRFQT, SVM-Short with peak value 1.159, position of peak 235, region range of SVM-Short, SVM-Joint 232-248, 229-246, 84-97. The plot of SVM-All is shown in the red line, SVM-Long in Blue, and SVM-Short in Yellow with the X-axis of sequence position, and Y-axis of domain linker prob in DLP are shown in Figure 4 (Karp et al., 2002), and the DLD1 protein profiling was based on given protein sequence, principally used via these profile based studies; deep conventional neural network, features, and combine similarity-based function such as cellular, biological and molecular-based functionality of the DLD1 gene are shown in Table 2.

Table 02: The DLD1 Predicted Protein Functions in AD

Cellular Component
GO:0005575 - cellular component - 0.812
GO:0005623 - cell - 0.812
GO:0044464 - cell part - 0.812
GO:0005622 - intracellular - 0.773
GO:0044424 - intracellular part - 0.773
GO:0005737 - cytoplasm - 0.772
GO:0044444 - cytoplasmic part - 0.772
GO:0043226 - organelle - 0.574
GO:0043229 - intracellular organelle - 0.573
GO:0043227 - membrane-bounded organelle - 0.534
GO:0005739 - mitochondrion - 0.505
GO:0043231 - intracellular membrane-bounded organelle - 0.505
GO:0032991 - macromolecular complex - 0.412
GO:0043234 - protein complex - 0.354
GO:0044422 - organelle part - 0.347
GO:0044446 - intracellular organelle part - 0.346
Molecular Function
GO:0003674 - molecular function - 0.737
GO:0003824 - catalytic activity - 0.722
GO:0016491 - oxidoreductase activity - 0.665
GO:0016651 - oxidoreductase activity, acting on NAD(P)H - 0.418
GO:0005488 - binding - 0.324
GO:0043167 - ion binding - 0.324
GO:0016667 - oxidoreductase activity, acting on a sulfur group of donors - 0.323

GO:0016668 - oxidoreductase activity, acting on a sulfur group of donors, NAD(P) as acceptor - 0.307
Biological Process
GO:0008150 - biological process - 0.822
GO:0008152 - metabolic process - 0.771
GO:0044699 - single-organism process - 0.756
GO:0044710 - single-organism metabolic process - 0.756
GO:0055114 - oxidation-reduction process - 0.672
GO:0044281 - small molecule metabolic process - 0.664
GO:0009987 - cellular process - 0.618
GO:0044237 - cellular metabolic process - 0.618
GO:0006807 - nitrogen compound metabolic process - 0.583
GO:0071704 - organic substance metabolic process - 0.583
GO:1901564 - organonitrogen compound metabolic process - 0.583
GO:0044763 - single-organism cellular process - 0.561
GO:0006082 - organic acid metabolic process - 0.500
GO:0043436 - oxoacid metabolic process - 0.491
GO:0019752 - carboxylic acid metabolic process - 0.486
GO:0044238 - primary metabolic process - 0.459
GO:0009058 - biosynthetic process - 0.420
GO:0044711 - single-organism biosynthetic process - 0.420
GO:0006793 - phosphorus metabolic process - 0.380
GO:0034641 - cellular nitrogen compound metabolic process - 0.372
GO:1901576 - organic substance biosynthetic process - 0.356
GO:1901360 - organic cyclic compound metabolic process - 0.351
GO:0046483 - heterocycle metabolic process - 0.340
GO:0044249 - cellular biosynthetic process - 0.335
GO:0019637 - organophosphate metabolic process - 0.332
GO:0006732 - coenzyme metabolic process - 0.317
GO:0051186 - cofactor metabolic process - 0.317
GO:0006139 - nucleobase-containing compound metabolic process - 0.313
GO:0006725 - cellular aromatic compound metabolic process - 0.313
GO:0055086 - nucleobase-containing small molecule metabolic process - 0.313
GO:0006753 - nucleoside phosphate metabolic process - 0.307
GO:0006796 - phosphate-containing compound metabolic process - 0.307
GO:0009117 - nucleotide metabolic process - 0.307

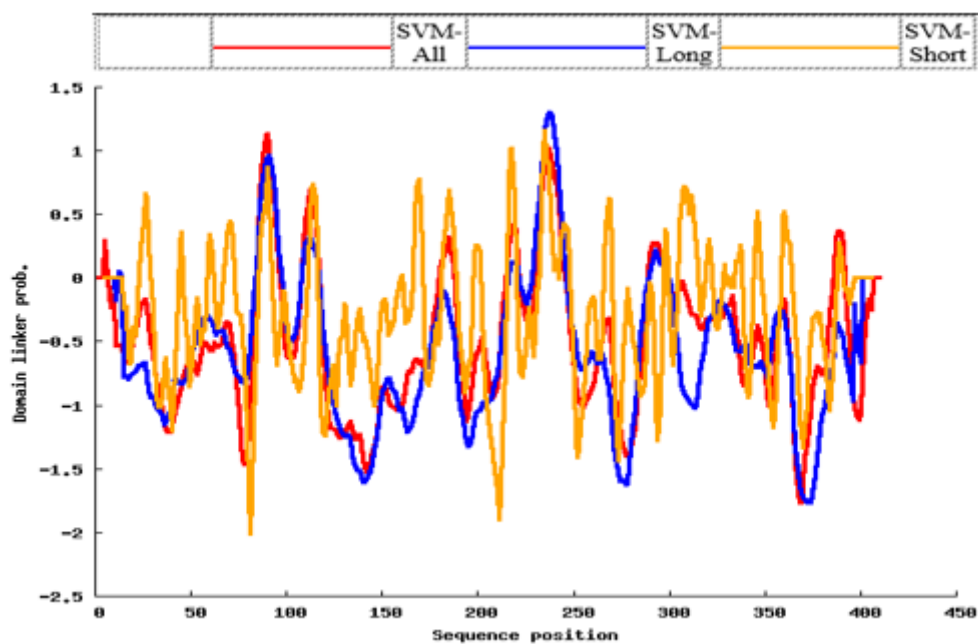


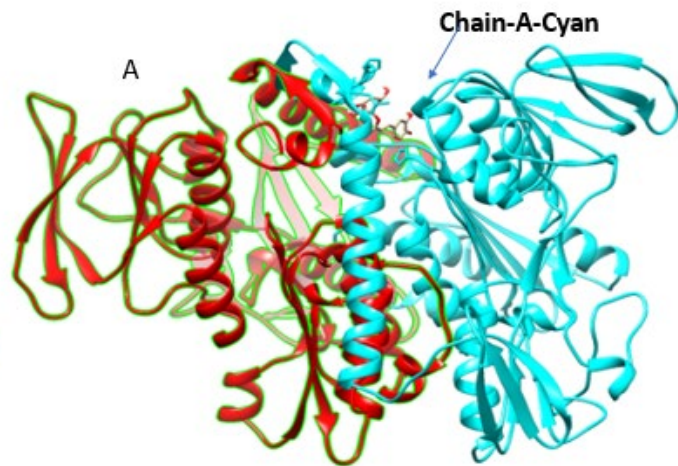
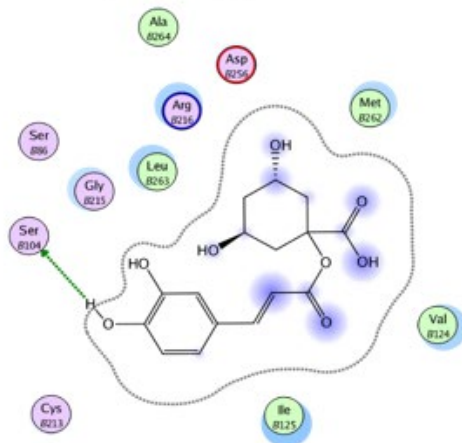
Figure 4: SVM domain protein analysis of the DLD1 in AD favorite candidate region (-1.5-1.5) prediction

4.4 Molecular Docking of DLD1

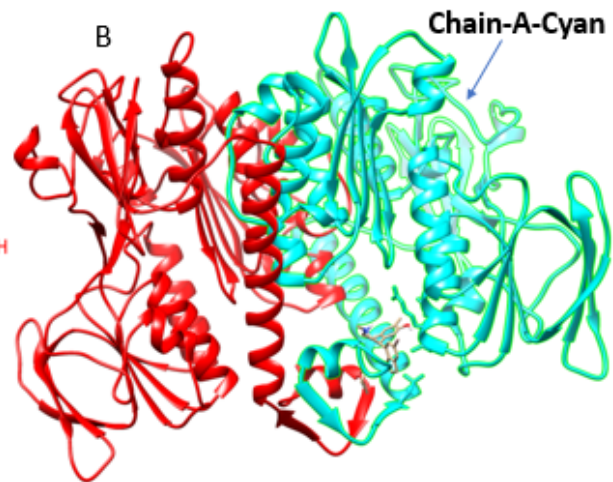
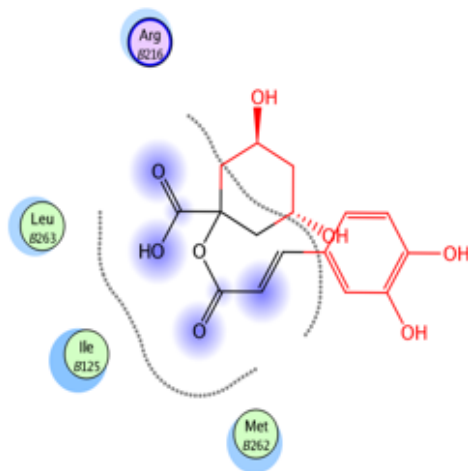
A comprehensive library of 15,282 natural compounds from traditional-herbal Chinese medicinal plants was docked against DLD1 in AD, and the top ten hits of phytochemicals with chain-A binding pocket residues were screened out. The selection criteria were based on the occupancy of binding pocket residues domain residual type-A with maximum binding affinity, high RMSD, least gibbs free energy, and minimum energy function score. Noticeably these selected top compounds showed minimum binding energy between -13.7117kcal/mol and -10.4600kcal/mol. Out of 15,282 medicinal-phytochemicals, the three best poses/hits such as 1-Caffeoyl-4-deoxyquinic acid (Arg216, Leu263, Ile125, Met262), N-Butyryl Coenzyme A (Arg216, Leu263, Ile125, Met262), Precatorine (Met262, Asp256, Leu263). The top 03 possible hits against the targeted protein of DLD1 in AD; (*Arg216, Leu263, Ile125, Met262, Asp256*), were selected based on minimum scoring function (-13.7117, -12.4565, -11.6440), with the RMSD-refine values (1.64, 0.86, 0.93), are shown in Table 3 with maximum interactive binding top three complex of DLD1 in AD of Chain-A were selected on the basis of binding affinities, S-docking scores via; complex1: 1-Caffeoyl-4-deoxyquinic acid, complex2: N-Butyryl Coenzyme A, and complex3: Precatorine highly binding pockets residues were selected through PyRx Docking Tool [62] in chain-A (ARG216, LEU263,

ILE125, MET262, ASP256) with including phytochemical names, class, and plants name of phytochemicals, also domains of predicted protein through Pfam-tool ranges between protein domains values are 42 to 410 from start to end domains are shown in , the most interactive residue of complex1: 1-Caffeoyl-4-deoxyquinic acid, complex2: N-Butyryl Coenzyme A, and Complex3: Precatorine are shown in Figure 5.

1-Caffeoyl-4-deoxyquinic acid



N-Butyryl Coenzyme A



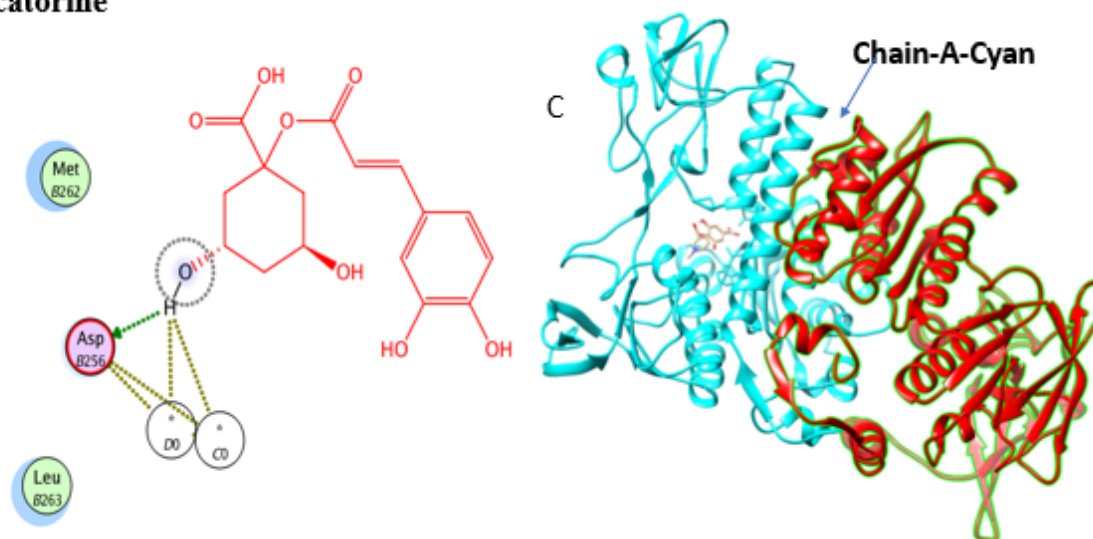
Precatorine

Figure 05: The top 03 compounds visualized residues-interaction (Chain-A-Cyan) of DLD1 in AD

Table 03: Interaction detail of top 03 bioactive phytochemicals, plant name, phytochemical name, class, S-scores, and RMSD-values with interactive residue against DLD1 in AD

Sr no	Ligands ID	Chemical Name	Plant name	Phytochemical name	Class	Docking Score (S)	Rmsd value	Residues
1	5281760	1-Caffeoyl-4-deoxyquinic acid	Chod et Hassl	Caffeoylquinic acid	Cinnamic acid	-13.7117	1.6432	Arg216 Leu263 Ile125 Met262
2	265	N-Butyryl Coenzyme A	Auxin Family	Butanoic acid	Butyrate	-12.4565	0.8606	Arg216 Leu263 Ile125 Met262
3	54704420	Precatorine	Abrus precatorius-Linn	<i>N-Dimethyl-L-tryptophan</i>	Alkaloids	-11.6440	0.9397	Met262 Asp256 Leu263

4.5 Pharmacokinetics analysis

ADMET drug-likeness analysis of selected top ten phytochemicals was performed through molinspiration (Ubani et al., 2020) based on the Lipinski rule of five (Ro5). The screened top-

phytochemicals displayed no violations to Lipinski's Ro5 and exhibited acceptable drug-like properties like HBA (8,2,6), HBD (5,2,1), MloP values (0.24,1.49,-5.26) are shown in Table 4.

Table 04: Lipinski rule of five of DLD1 gene in AD

Compounds	Molecular weight (g/mol)	Number of HBA	Number of HBD	MLogP
Lipinski's rule of five	<500	<10	<5	<5
1-Caffeoyl-4-deoxy quinic acid	338.31	8	5	0.24
N-Butyryl Coenzyme A	409.73	2	2	1.49
Precatorine	288.24	6	1	-5.26

Furthermore, pharmacokinetic properties were predicted through the SwissADME server for the validation of phytochemicals' drug-likeness (GI-absorption, BBB permeant, P-gp substrate, CYP1A2, CYP2C19, CYP2C9, CYP2D6, CYP3A4-inhibitors, Log K_p, Ghose, Veber, Egan, Muggli, bioactivity scores, sub-cellular localization of the top-hits against the DLD1) are shown in Table 5.

Table 05: Prediction of top 03 compounds ADMETSAR of DLD1 in AD

Compounds	1-Caffeoyl-4-deoxy quinic acid	N-Butyryl Coenzyme A	Precatorine
GI absorption	Low	High	High
BBB permeant	No	Yes	No
P-gp substrate	No	Yes	No
CYP1A2 inhibitor	No	Yes	Yes
CYP2C19 inhibitor	No	No	No
CYP2C9 inhibitor	No	Yes	No
CYP2D6 inhibitor	No	No	No
CYP3A4 inhibitor	No	No	No
Log K _p (skin permeation)	-7.97	-5.48	-7.20
Ghose	Yes	Yes	Yes

Veber	No, TPSA>140	Yes	Yes
Egan	No, TPSA>131.6	Yes	Yes
Muegge	Yes	Yes	Yes
Bioavailability Score	0.56	0.55	0.56
Subcellular localization	Mitochondria	Mitochondria	Mitochondria

Next, a toxicity assessment of the top 10 ranked potential compounds was obtained after the docking analysis with different toxicity modules. These selected top compounds' bioactivities results (GPCR-Ligands, ion channel modulators, a kinase inhibitor, nuclear receptor ligand, protease inhibitor, and enzymatic inhibitors) are shown in Table 6.

Table 06: Prediction of top 03 compounds Bioactivity

Compound name	GPCR Ligand	Ion channel modulator	Kinase inhibitor	Nuclear receptor ligand	Protease inhibitor	Enzyme inhibitor
1-Caffeoyl-4-deoxy quinic acid	0.28	0.17	-0.01	0.82	0.25	0.63
N-Butyryl Coenzyme A	0.26	0.24	-0.12	0.07	-0.32	0.19
Precatorine	-0.05	0.36	-0.45	-1.0	-0.17	0.20

Our analysis revealed that these top three complexes tend to bind targeted regions of DLD1 in Alzheimer's disease and are validated subsequently via MD simulation. the enzymatic associated properties of the DLD1 in AD have also been revealed such as; acetyl CoA biosynthesis, the citric acid cycle also called the TCA cycle, glycine metabolism, oxidative decarboxylation of pyruvate and other properties are shown in Table no 7.

Table no 07: The enzymatic association properties of DLD1 in AD

Enzymatic interaction	
Substrate products	330
Natural substrates	58
Cofactors	197
inhibitors	100
Functional Parameters	
KM values	228
Turnover numbers	67

Kcat values	08
Ki values	32
IC50 values	10
Specific activity	76
PH optima	46
PH range	09
pI values	04
Molecular Properties	
pH stability	02
General stability	03
Expression	02
Renatured	01

4.6 MD-Simulation of DLD1 in AD

MD simulations were carried out following the docking with the Desmond Simulation Package for 100 ns per complex. MD trajectories calculated the RMSD values, the root-mean-square fluctuation values, and the protein-ligand interaction values. Results were shown to be reproducible from a simulation for each complex and are shown below.

4.6.1. RMSD Analysis

The stability of the modeled proteins was verified by plotting the root mean square deviation (RMSD) graph for backbone atoms during the production run. The RMSD for the complex of DLD1 with 1-Caffeoyl-4-deoxyquinic acid continued to show minimal deviation till 20 ns and achieved stability until the end of 50 ns (Fig. 2A). Similarly, the RMSD plot for the complex of DLD1 with N-Butyryl Coenzyme A showed the fluctuation of 0.1 nm up to 20ns and showed the stable trajectory throughout the production run (Fig. 2B). On the contrary, the complex of DLD1 with Precatorine exhibited a stable trajectory up to 10 ns. Later to 10 ns a small deviation of 0.1 nm was observed while the complex remained stable throughout the simulation period (Fig. 2C).

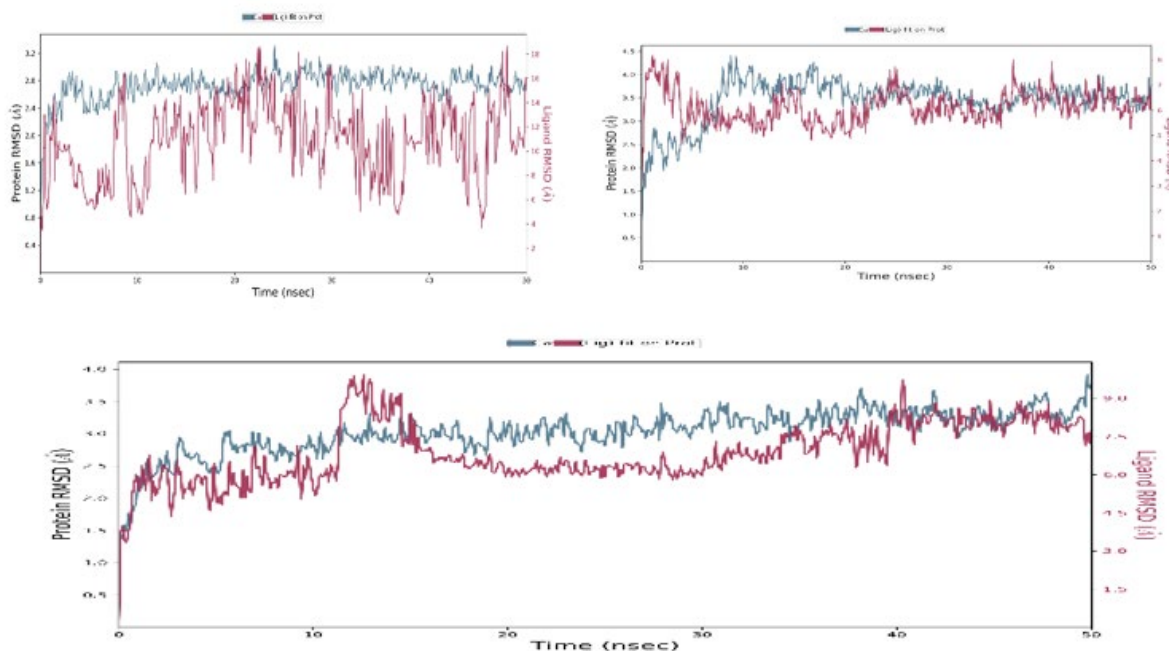


Figure 2. MD simulation interaction diagrams of 50 ns trajectory showing RMSD: RMSD plot of complex DLD1 protein with three ligands, 1-Caffeoyl-4-deoxyquinic acid (A), N-Butyryl Coenzyme A (B) and Precatorine (C), respectively. The RMSD trajectories of the backbone atoms for the protein are shown in blue and the ligand in red.

4.6.2. RMSF Analysis

The RMSF of individual amino acid residues of the protein was calculated during the entire simulation process to ascertain the flexibility of the protein system Figure 3((A), (B), and (C)). The RMSF ranged from 0.6 to 4.8 Å, 0.8 to 5.6 Å, and 0.6 to 5.4 Å, for DLD1-1-Caffeoyl-4-deoxyquinic acid complex, DLD1-N-Butyryl Coenzyme A complex, and Precatorine complex respectively demonstrating a stable protein-ligand complex. RMSF is positively stable in the three complexes with the fluctuation maxima between residues no. 50-80, 450-470, and 490-500 for 1-Caffeoyl-4-deoxyquinic acid, N-Butyryl Coenzyme A, and Precatorine respectively. However, some other deviations between residues no. 440-450 and 490-495 for 1-Caffeoyl-4-deoxyquinic acid, and 75-85, 490-500 for N-Butyryl Coenzyme A, 30-40, 400-410 with Ligand 15 were observed during simulation of DLD1 with respective ligands (Figure 3((A), (B) and (C)).

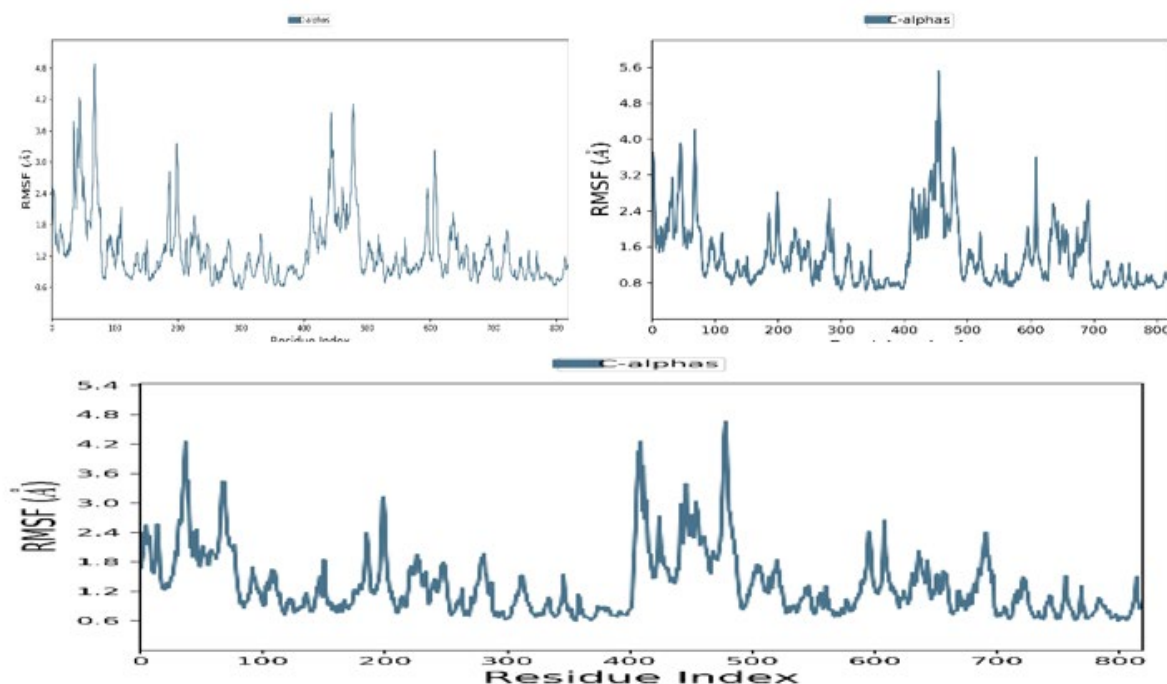


Figure 3. Protein Root Mean Square Fluctuation (RMSF) plots (Angstrom). (A) RMSF trajectory plot of DLD1-1-Caffeoyl-4-deoxyquinic acid complex showing residue-wise fluctuation (B) RMSF trajectory plot for DLD1-N-Butyryl Coenzyme A complex showing residue-wise fluctuations (C) RMSF trajectory plot of DLD1-Precatorine complex showing residue-wise fluctuation. The average RMSF for DLD1-1-Caffeoyl-4-deoxyquinic acid complex, DLD1-N-Butyryl Coenzyme A complex, and DLD1-Precatorine complex were 2.7 Å, 3.1 Å, and 2.75 Å respectively.

The average RMSF for DLD1-1-Caffeoyl-4-deoxyquinic acid complex, DLD1-N-Butyryl Coenzyme A complex, and DLD1-Precatorine complex were 2.7 Å, 3.1 Å, and 2.75 Å respectively.

4.6.3. Protein-Ligand interaction analysis

Protein-ligand contact profiles for the DLD1 complex with 1-Caffeoyl-4-deoxyquinic acid, N-Butyryl Coenzyme A, and Precatorine were also accessed from the simulation trajectories as shown in Figure 3(A,B and C). The two residues' LYS_28 and GLU_128 exhibited hydrogen bonds for the DLD1-1-Caffeoyl-4-deoxyquinic acid protein-ligand complex, and various hydrophobic interactions with MET_1, HIS_3, LEU_19, MET_24, VAL132, ARG_135, LEU136, and HIS_297. The residues HIS_3, LYS_28, GLU_128, TYR_295, and ASN_33 contributed to the formation of water bridges (Figure 4(A)).

It was observed that the N-Butyryl Coenzyme A interacted with LYS_28, MET_1, HIS_297, and ARG_10 mainly through ionic interaction. Hydrogen bond interactions with MET_1, ALA_2, HIS_3, VAL_17, ARG_10 and ARG_135 and various water bridges with residues MET_1, ALA_2, HIS_3, GLU_16, VAL_17, ARG_10, LYS_28 and SER_9 played a supportive role in binding the ligand. The hydrophobic interaction encompasses residues such as MET_1, VAL_17, LEU_19, MET_24, AGG_135, LEU_136 and ILE_12(Figure 4(B)).

For the protein-ligand complex DLD1-Precatorine, strong hydrogen bonds were formed by the residues such as ARG_235, ARG_237, TYR_287, and ASN_288, while VAL_152, PRO_261, TYR_287, and TRP_302, ALA-910 are five amino acid residues that contributed to strong hydrophobic interactions. The residues ARG_237 and LYS_305 established the ionic interaction with the related ligand atoms (Figure 4(C)).

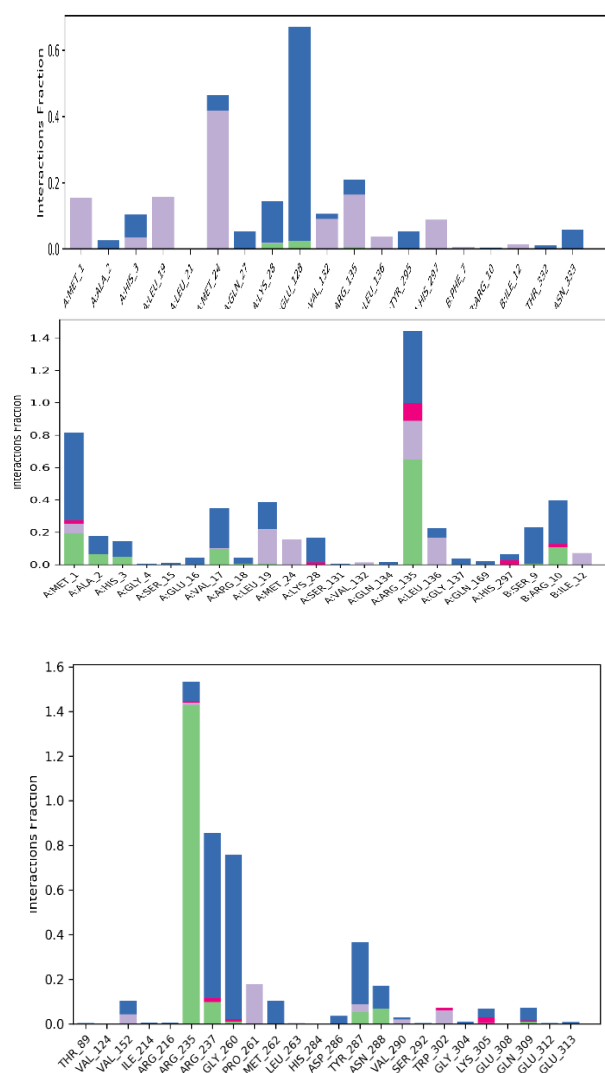


Figure 4. Protein-ligand contact interaction profile analyzed for (A) DLD1-1-Caffeoyl-4-deoxyquinic acid complex, (B) DLD1-N-Butyryl Coenzyme A complex, and (C) DLD1-Precatorine complex calculated during 50 ns MD simulation. The green color =hydrogen bonding, the pink color ionic interaction, the white darker color = hydrophobic interaction, and the blue color = water bridges.

4.6.4. Radius of gyration (Rg) and solvent accessible surface area (SASA)

For the assessment of the nature of biological molecules and stability during MD time, the radius of gyration (Rg) was computed. Figure 5(A, B & C) displays Rg values of the complex DLD1-1-Caffeoyl-4-deoxyquinic acid complex, DLD1-N-Butyryl Coenzyme A complex, and DLD1-Precatorine complex during the MD trajectory pose. The Rg values through the simulation at 50 ns of DLD1-1-Caffeoyl-4-deoxyquinic acid complex, DLD1-N-Butyryl Coenzyme A complex and DLD1-Precatorine complex were $0.004 \text{ nm} \pm 0.016 \text{ nm}$, $0.32 \text{ nm} \pm 0.48 \text{ nm}$, and $0.037 \text{ nm} \pm 0.48$ respectively (Figure 5A, B & C).

Solvent accessible surface area (SASA) analysis measures the interaction between complexes and solvents. The estimated average range SASA values of the complex DLD11-Caffeoyl-4-deoxyquinic acid complex, DLD1-N-Butyryl Coenzyme A complex, and DLD1-Precatorine complex for 50 ns simulation were between the $1.2 \pm 3 \text{ nm}$, 1.0 ± 2.0 , and $2.00 \pm 4.0 \text{ nm}$ respectively as depicted in Figure 5(D, E & F). the results suggest that it should be accessible for solvents and have more interaction with solvents. In addition, SASA values for the three protein complexes remained stable during the MD simulation run.

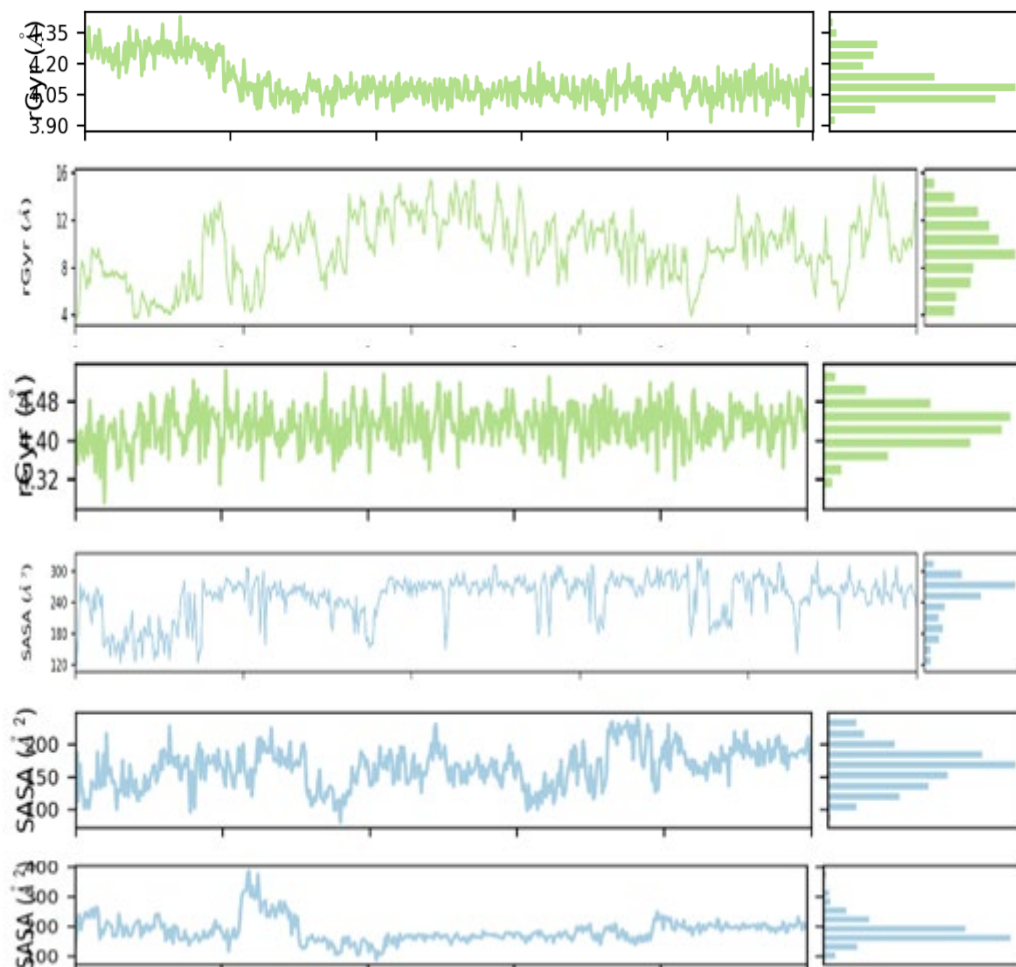


Figure 5. The time frame evolution against the radius of gyration (Rg) (A, B & C) and the SASA plots of docked complexes over 50 ns MD simulation (D, E & F).

5 Conclusion

DLD1 is one of the vital enzymatic proteins involved in regulating neural activities, cognitive behaviors, signaling, and progression of energy metabolisms. The excessive activity of DLD1 enzymes in patients of AD leads to dementia as well as neural activity disturbances. Therefore, in our research, we sought to identify the potential hits drug compounds from medicinal plants, and bioactive compounds (1-Caffeoyl-4-deoxyquinic acid, N-Butyryl Coenzyme A, Precatorine) were docked that could help suppress the activity of DLD1. The selection of the top three compounds is based on their minimum energy function score, maximum occupancy with binding pocket residues, binding energies, and least RMSD. Our analysis also showed that the top ten selected phytochemicals also have binding affinities with the conserved domain of

chain-A residues of DLD1 However, *in-vivo* and *in-vitro* analysis has to be required to use these potential compounds against Alzheimer's disease.

Conflict of interest: The authors declare no conflict of interest.

Ethical approval: Not applicable.

References:

- Ballatore, C., Lee, V. M.-Y., & Trojanowski, J. Q. (2007). Tau-mediated neurodegeneration in Alzheimer's disease and related disorders. *Nature Reviews Neuroscience*, 8(9), 663-672.
- Brown, A. M., et al. (2007). Testing for linkage and association across the dihydrolipoyl dehydrogenase gene region with Alzheimer's disease in three sample populations. *Neurochemical Research*, 32(4-5), 857-869.
- Carothers, D. J., Pons, G., & Patel, M. S. (1989). Dihydrolipoamide dehydrogenase: functional similarities and divergent evolution of the pyridine nucleotide-disulfide oxidoreductases. *Archives of Biochemistry and Biophysics*, 268(2), 409-425.
- Eleazu, C., et al. (2012). Comparative study of the phytochemical composition of the leaves of five Nigerian medicinal plants. *Journal of Biotechnology and Pharmaceutical Research*, 3(2), 42-46.
- Giuffrida, M. L., et al. (2009). β -amyloid monomers are neuroprotective. *Journal of Neuroscience*, 29(34), 10582-10587.
- Grassi, B., et al. (1998). Faster adjustment of O₂ delivery does not affect V_{o2} on-kinetics in isolated in situ canine muscle. *Journal of Applied Physiology*, 85(4), 1394-1403.
- Hoyer, S. (2004). Glucose metabolism and insulin receptor signal transduction in Alzheimer disease. *European Journal of Pharmacology*, 490(1-3), 115-125.
- Hoyer, S., & Nitsch, R. (1989). Cerebral excess release of neurotransmitter amino acids subsequent to reduced cerebral glucose metabolism in early-onset dementia of Alzheimer type. *Journal of Neural Transmission*, 75(3), 227-232.
- Ling, Y., Morgan, K., & Kalsheker, N. (2003). Amyloid precursor protein (APP) and the biology of proteolytic processing: relevance to Alzheimer's disease. *The International Journal of Biochemistry & Cell Biology*, 35(11), 1505-1535.
- Mattson, M. P., Gleichmann, M., & Cheng, A. (2008). Mitochondria in neuroplasticity and neurological disorders. *Neuron*, 60(5), 748-766.
- Mukhtar, M., et al. (2008). Antiviral potentials of medicinal plants. *Virus Research*, 131(2), 111-120.
- Nag, S., et al. (2011). Nature of the amyloid- β monomer and the monomer-oligomer equilibrium. *Journal of Biological Chemistry*, 286(16), 13827-13833.
- Ott, A., et al. (1999). Diabetes mellitus and the risk of dementia: The Rotterdam Study. *Neurology*, 53(9), 1937-1937.
- Perry, T., & Greig, N. H. (2002). The glucagon-like peptides: a new genre in therapeutic targets for intervention in Alzheimer's disease. *Journal of Alzheimer's Disease*, 4(6), 487-496.
- Reitz, C., & Mayeux, R. (2014). Alzheimer disease: epidemiology, diagnostic criteria, risk factors and biomarkers. *Biochemical Pharmacology*, 88(4), 640-651.
- Ristow, M. (2004). Neurodegenerative disorders associated with diabetes mellitus. *Journal of Molecular Medicine*, 82(8), 510-529.

- Shi, Q., et al. (2008). Novel functions of the α -ketoglutarate dehydrogenase complex may mediate diverse oxidant-induced changes in mitochondrial enzymes associated with Alzheimer's disease. *Biochimica et Biophysica Acta (BBA)-Molecular Basis of Disease*, 1782(4), 229-238.
- Sun, M.-K., & Alkon, D. L. (2006). Links between Alzheimer's disease and diabetes. *Drugs of Today*, 42(7), 481.
- Taylor, M., et al. (2010). Development of a proteolytically stable retro-inverso peptide inhibitor of β -amyloid oligomerization as a potential novel treatment for Alzheimer's disease. *Biochemistry*, 49(15), 3261-3272.
- Vilalta, A., & Brown, G. C. (2014). Deoxyglucose prevents neurodegeneration in culture by eliminating microglia. *Journal of Neuroinflammation*, 11(1), 1-10.
- Völgyi, K., et al. (2017). Mitochondrial proteome changes correlating with β -amyloid accumulation. *Molecular Neurobiology*, 54(3), 2060-2078.
- Wang, D., et al. (2015). Role of intestinal microbiota in the generation of polyphenol-derived phenolic acid mediated attenuation of Alzheimer's disease β -amyloid oligomerization. *Molecular Nutrition & Food Research*, 59(6), 1025-1040.
- Wang, J., et al. (2014). Cocoa extracts reduce oligomerization of amyloid- β : implications for cognitive improvement in Alzheimer's disease. *Journal of Alzheimer's Disease*, 41(2), 643-650.
- Wang, J.-Z., et al. (2013). Abnormal hyperphosphorylation of tau: sites, regulation, and molecular mechanism of neurofibrillary degeneration. *Journal of Alzheimer's Disease*, 33(s1), S123-S139.
- Wimo, A., et al. (2017). The worldwide costs of dementia 2015 and comparisons with 2010. *Alzheimer's & Dementia*, 13(1), 1-7.
- Yadav, R., & Agarwala, M. (2011). Phytochemical analysis of some medicinal plants. *Journal of Phytology*.
- Yao, J., et al. (2011). 2-Deoxy-D-glucose treatment induces ketogenesis, sustains mitochondrial function, and reduces pathology in female mouse model of Alzheimer's disease. *PLOS One*, 6(7), e21788.
- Zhang, H., et al. (2012). Proteolytic processing of Alzheimer's β -amyloid precursor protein. *Journal of Neurochemistry: REVIEW*, 120, 9-21.
- Zhang, L.-F., et al. (2015). Coffee and caffeine potentiate the anti-amyloidogenic activity of melatonin via inhibition of A β oligomerization and modulation of the Tau-mediated pathway in N2a/APP cells. *Drug Design, Development and Therapy*, 9, 241.
- Zhang, Y.-w., et al. (2011). APP processing in Alzheimer's disease. *Molecular Brain*, 4(1), 1-13.